DIAGRAMS OF CRITICAL EQUILIBRIUM FOR BRITTLE BODIES WITH SHARP FLAWS

L. L. Libatskii and V. V. Panasyuk

Certain forms of the stress-intensity factors close to the tips of sharp flaws (plane problem) are used as the basis of a method for plotting critical equilibrium diagrams for brittle bodies with flaws in the form of pointed cavity-cracks [5]. Concrete examples are discussed, mainly in the context of such diagrams, for a brittle body weakened by a circular cavity flaw with a crack leaving the edge of the flaw. Determination of the stress-intensity factors for this problem is based on approximate solution of an integral equation by the method of collocations. Plots of some familiar diagrams are also analyzed.

1. Equations of the Critical Stress Diagrams. Consider a two-dimensional brittle body weakened by sharp stress raisers (with cusps of the first kind). Let the raisers be so far apart that their interaction is negligible. Let the origin of polar coordinates r, θ be located at the tip of one raiser, with θ measured from the tangent to the raiser contour at the tip. Then the component σ_θ of the elastic fracture stresses in the neighborhood of the tip (i.e., with r small) can be written as [1-5]

$$\sigma_\theta = \frac{N}{\sqrt{r}} + O(1), \quad N = {}^1/_2 \sqrt{2} \cos^2 \theta/2 \, (k_1 \cos \theta/2 - 3k_2 \sin \theta/2) \tag{1.1}$$

Here, k_1 and k_2 are the stress-intensity factors due respectively to the symmetric and antisymmetric (relative to the tangent at the raiser tip) parts of the external load, and O(1) is the part of the stress component that is bounded as $r \to 0$.

The body reaches its critical equilibrium state when [2, 3, 5]

$$N_{\max} = K/\pi \qquad \text{(K is modulus of cohesion)} \tag{1.2}$$

Let the body be loaded "at infinity" by two mutually perpendicular stresses p and q ($p \geq q$), in such a way that p forms an angle α with the tangent at the raiser tip. With this type of external load and the class of stress raiser in question, the stress-intensity factors can be written as

$$k_1 = (p+q)f_1 - (p-q)f_2 \cos 2\alpha, \quad k_2 = (p-q)f_3 \sin 2\alpha \tag{1.3}$$

where f_1, f_2, and f_3 are functions of the geometric parameters of the raiser (it will be assumed henceforth for simplicity that $f_1 > 0$ and $f_2 > 0$).

Substituting (1.3) in (1.1) and equating the derivative $\partial N/\partial\alpha$ to zero,

$$\mathrm{tg} 2\alpha = (3f_3/f_2)\, \mathrm{tg}\, \theta/_2$$

Hence

$$\cos 2\alpha = \pm \frac{f_2 \cos \theta/2}{\sqrt{9f_3^2 \sin^2 \theta/2 + f_2^2 \cos^2 \theta/2}} \tag{1.4}$$

Using (1.1), (1.3), and (1.4), the second derivative $\partial^2 N/\partial\alpha^2$ is seen to be negative if the lower sign is taken in (1.4) (and in the similar expression for $\sin 2\alpha$). The expression for the maximum of N as a function of α is then

---

L'vov. Translated from Prikladnoi Mekhaniki i Tekhnicheskoi Fiziki, Vol. 11, No. 3, pp. 98-104, May-June, 1970. Original article submitted March 10, 1969.

$$N_{\max}^{(\alpha)} = {}^1/_4\,(1+\cos\theta)\,[(p+q)\,f_1\sqrt{1+\cos\theta}+(p-q)\sqrt{2\,(A-B\cos\theta)}]$$
$$2A = 9f_3^2+f_2^2, \qquad 2B = 9f_3^2-f_2^2 \qquad (1.5)$$

Now consider the extremum of (1.5) as a function of θ. Equating the derivative $dN_{\max}^{(\alpha)}/d\theta$ to zero,

$$\sin\theta\left[3\,(p+q)\,f_1\sqrt{1+\cos\theta}+\sqrt{2}\,(p-q)\,\frac{2A-B-3B\cos\theta}{\sqrt{A-B\cos\theta}}\right]=0 \qquad (1.6)$$

Equating the first factor on the left of (1.6) to zero yields $\theta = 0$ (the values $\theta = \pm\pi$ are discarded from physical considerations). With this value of θ, the second derivative will be negative if

$$F(p,q) = [f_2(f_1+f_2)-3f_3^2]p + [f_2(f_1-f_2)+3f_3^2]q > 0 \qquad (1.7)$$

Assuming that condition (1.7) is satisfied, and putting $\theta = 0$ in (1.5),

$$N_{\max}^{(1)} = {}^1/_2\sqrt{2}[(f_1+f_2)p+(f_1-f_2)q] \qquad (1.8)$$

Equating to zero the expression in brackets on the left of (1.6) gives

$$\cos\theta = \frac{1}{F_3}\{(A-B)\,F_1+4B^2\,(p-q)^2+(A+B)\,F_2\} \qquad (1.9)$$

where

$$F_1 = 8B(p-q)^2+3(p+q)^2f_1^2, \quad F_3 = 6B[2B(p-q)^2+(p+q)^2f_1^2]$$
$$F_2 = (p+q)\,f_1\sqrt{9\,(p+q)^2f_1^2+16B\,(p-q)^2}$$

and the absolute value is considered under the square root sign. For the values of θ given by (1.9), the second derivative $d^2N_{\max}^{(\alpha)}/d\theta^2$ will be negative if

$$F(p,q) < 0$$

where the function F is given by (1.7). Substitution of (1.9) for $\cos\theta$ in (1.5) gives

$$N_{\max}^{(2)} = (A+B)^{3/2}\frac{F_1+F_2}{4F_3}\left\{(p+q)\,f_1\left(\frac{F_1+F_2}{F_3}\right)^{1/2}\right.$$
$$\left.+\,(p-q)\left(\frac{2B}{F_3}\,[F_1-4B\,(p-q)^2-F_2]\right)^{1/2}\right\} \qquad (1.10)$$

The critical equilibrium condition (1.2) may thus be written in the form of two equations:

$$(f_1+f_2)\,p_*+(f_1-f_2)\,q_* = \frac{\sqrt{2}K}{\pi}, \quad F\,(p_*,\,q_*)>0 \qquad (1.11)$$

$$(A+B)^{3/2}\frac{F_1+F_2}{2\sqrt{2}F_3}\left\{(p_*+q_*)\,f_1\left(\frac{F_1+F_2}{F_3}\right)^{1/2}\right.$$
$$\left.+\,(p_*-q_*)\left(\frac{2B}{F_3}\,[F_1-4B\,(p_*-q_*)^2-F_2]\right)^{1/2}\right\} = \frac{\sqrt{2}K}{\pi} \quad F\,(p_*,\,q_*)<0 \qquad (1.12)$$

Here, p_* and q_* are the least values of the external stresses for which (1.2) is satisfied (the critical stresses [5, 6]). Equations (1.11) and (1.12) define a line in the pq plane, termed in [5] the critical stress diagram. Obviously, if $q \geq p$, the diagram is simply reflected in the bisector of the first and third quadrants. If the stressed state in a body with the type of flaws in question is such that the point with coordinates p, q lies inside the region bounded by the diagram (i.e., is located on the sample side as the origin of the pOq coordinate system), the safety factor in the body will be greater than unity; otherwise, it is less than unity. If the point (p, q) lies on the diagram, the equilibrium state of the body is critical in the sense that the slightest additional load (taking the point into the outer region) will cause fracture to commence.

It is more convenient to plot these strength diagrams in the relative coordinates

$$x^\circ = p/\sigma_B, \qquad y^\circ = q/\sigma_B$$

where σ_B is the engineering strength of the body, which will be assumed [5] equal to the least critical external load $\sigma_B = p_*$ ($q_* = 0$) in the case of one-sided extension of the body.

2. Analysis of Plots of Some Familiar Diagrams. 1. Let the body be weakened by isolated straight narrow slit-cracks of length $2\,l$. In this case,

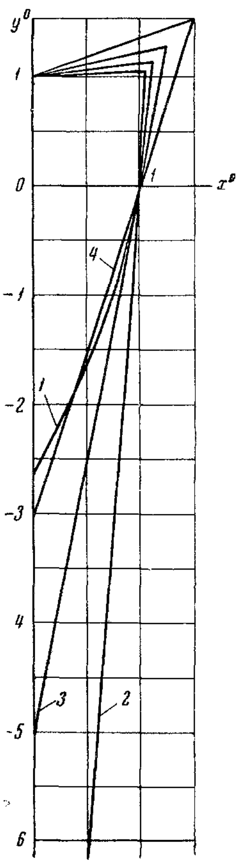

Fig. 1

$$f_1 = f_2 = f_3 = {}^1/_2 \sqrt{l}$$

Substitution of these values in (1.12) with $q_* = 0$ gives

$$p_* = \sigma_B = 0.97\pi^{-1} \sqrt{2/lK} \tag{2.1}$$

Recalling (1.12), it can now be seen that, in the first quadrant, from the line $y^\circ = x^\circ$ to the line $y^\circ = x^\circ/3$, the strength diagram is likewise a straight line: $x^\circ = 1.03$.

By using (1.12) and (2.1), sufficient points can be obtained for plotting the curved part of the diagram. For instance, with $s_1 = q_* / p_* = -1$, the point with coordinates $x_1^\circ = -0.79, y_1^\circ = -0.79$ is obtained, and with $s_2 = -4$, the point $x_2^\circ = 0.43$, $y_2^\circ = 0.43$, $y_2^\circ = -1.73$. The diagram cuts the y° axis at $y_3^\circ = -2.67$. The diagram plotted on the basis of this working is represented by curve 1 of Fig. 1. Notice that the diagram for the same case was plotted by another method in [6].

2. If the flaws in the body consist of hypocycloidal cavities [7], it is found, after eliminating some misprints from [7], that

$$\begin{gathered}
f_1 = -f \frac{(n+1)t^2 + nt + n - 1}{t^3 - (n+1)t^2 - t - n + 1} \\
f_2 = 2f \frac{3nt^3 + (n^2+2)t^2 + (n^2-4)t + n^2 - 3n + 2}{(n^2 - n + 4)t^2 + 4(n-2)t + n^2 - 3n + 4} \\
f_3 = -f \frac{6t^3 - (10-n)t^2 - (n^2+2)t + 2(n-1)}{(n^2 - n + 4)t^2 + 4(n-2)t + n^2 - 3n + 4} \\
f = \frac{n+t-1}{n} \left(\frac{(1-t)a}{(n+1)t + n - 1} \right)^{1/2}, \quad t = \frac{2 - (1-\varepsilon)n}{2 + (1-\varepsilon)n} \\
\varepsilon = b/a \quad \left(\frac{n-2}{n} \leqslant \varepsilon \leqslant 1 \right)
\end{gathered} \tag{2.2}$$

where $n \geq 3$ is the number of vertices, and a and b are the radii of circles circumscribed about and inscribed in the flaw.

A variety of flaws consisting of sharp hypocycloidal cavities may be obtained by varying n and ε. The critical stress diagram for each concrete case of n and ε is obtained by using (2.2) and the method described.

a) Let $n = 3$. With $\varepsilon = 1/3$, the diagram for a hypocycloid is obtained [6]. In the $x^\circ Oy^\circ$ coordinate system it is the same as curve 1. Using (1.12) and (2.2), it can be shown that, when $n = 3$, the body has maximum strength under one-sided compression when $\varepsilon = 0.58$. In this case, f_1, f_2, and f_3 take the values

$$f_1 = 0.456\sqrt{a}, \quad f_2 = 0.537\sqrt{a}, \quad f_3 = 0.126\sqrt{a} \tag{2.3}$$

Hence, recalling (1.8) and (1.12),

$$p_* = \sigma_B = 1.006\pi^{-1}\sqrt{2/aK} \tag{2.4}$$

In the first quadrant of the $x^\circ y^\circ$ coordinate system, and up to the line $y^\circ = -107x^\circ$ in the fourth quadrant, the strength diagram is now given by

$$x^\circ - 0.0815y^\circ = 1 \tag{2.5}$$

Using (1.12), (2.3), and (2.4), ($x_1^\circ = 0.076$, $y_1^\circ = -11.33$) is obtained with $s_1 = -150$, and ($x_2^\circ = 0.052$, $y_2^\circ = -11.66$) with $s_2 = -250$.

The y° axis cuts the diagram at the point $y_3^\circ = -12.16$. The critical stress diagram plotted from these data is represented by curve 2 of Fig. 1.

As ε increases up to 1, diagrams are obtained approximating to the diagram for a circular flaw [13] (curve 4 of Fig. 1).

b) Let $n = 4$. In this case the body has maximum strength under one-sided compression if the flaws in it are characterized by the parameter $\varepsilon = 0.57$. The strength diagram for this body is given in the first and fourth quadrants by

$$x^\circ - 0.201y^\circ = 1$$

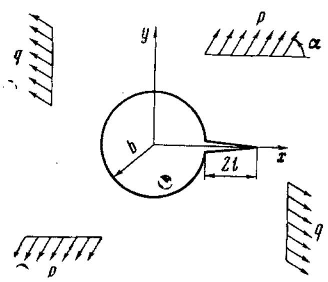

Fig. 2

The relevant diagram is marked 3 in Fig. 1. As in case a), diagrams approximating to the diagram for a circular flaw are obtained as $\varepsilon \to 1$.

3. Critical Stress Diagrams for a Circular Hole Plus Crack Type of Flaw. 1. Let the flaws in the body be represented by a circular hole of radius b and a crack of length $2l$, issuing from the hole boundary (Fig. 2). From [8-10], the problem on the stress-deformed state in a body with flaws of this kind may be reduced to solving the following system of two singular integral equations:

$$2D\int_0^1 M_i(\xi,\eta)\,\mu_i(\eta)\,d\eta + \Lambda_i^{(p)}(\xi) = 0$$
$$D = \frac{G}{\pi(1+\varkappa)}, \quad i = 1,2 \qquad (3.1)$$

Here, G is the shear modulus, $\varkappa = 3-4\nu$ or $\varkappa = (3-\nu)/(1+\nu)$ respectively in the cases of plane deformation or the plane stressed state, ν is Poisson's coefficient, and $\Lambda_1^{(p)} = \sigma_y^{(p)}$, $\Lambda_2^{(p)} = \tau_{xy}^{(p)}$ are respectively the normal and tangential components of the stresses due to the external load at the site of the crack when the plate is weakened solely by the circular hole. The kernels M_i of integral equations (3.1) are given by

$$M_1 = \frac{1}{\eta-\xi} + \frac{2\lambda(1+\lambda^2\xi^2)}{(1+\lambda\xi)^2}\left\{\frac{1}{1+\lambda\eta} + \frac{1}{1-\lambda\eta}\left[1 + \frac{2(1-\lambda\xi)}{(1+\lambda\xi)(1-\lambda\eta)}\right]\right\} - \frac{1}{\eta+\xi}\left\{1 - \frac{2\xi(1-\lambda\xi)}{(1+\lambda\xi)^2(\eta+\xi)}\left[\frac{3+\lambda^2\xi^2}{1+\lambda\xi} - \frac{2\xi(1-\lambda\xi)}{\eta+\xi}\right]\right\}$$
$$M_2 = \frac{1}{\eta-\xi} + \frac{8\lambda^2\xi}{(1+\lambda\xi)^3(1-\lambda\eta)}\left[\frac{2(1-\lambda\xi+\lambda^2\xi^2)}{1+\lambda\xi} + \frac{1-\lambda\xi}{1-\lambda\eta}\right] - \frac{(1-\lambda\xi)^2}{(1+\lambda\xi)^2(\eta+\xi)}\left\{\frac{(1-\lambda\xi)^2-8\lambda\xi}{(1+\lambda\xi)^2} - \frac{2\xi}{\eta+\xi}\left[\frac{3-\lambda\xi}{1+\lambda\xi} - \frac{2\xi}{\eta+\xi}\right]\right\} \qquad (3.2)$$
$$\left(\lambda = \frac{\varepsilon^\circ}{2+\varepsilon^\circ}, \quad \varepsilon^\circ = \frac{2l}{b}\right)$$

If the solutions of (3.1) are sought in the form [10]

$$\mu_i = -\frac{1}{2D}\left(\frac{k_i}{\pi\sqrt{2l(2+\varepsilon^\circ)(1-\eta)}} + \sqrt{1-\eta}\sum_{n=0}^{m} a_n^{(i)}\eta^n\right) \quad (i=1,2) \qquad (3.3)$$

it can be shown that the stress concentration in the neighborhood of the length of the crack is characterized by

$$\sigma_y = \frac{k_1}{\sqrt{2r}} + O(1), \qquad \tau_{xy} = \frac{k_2}{\sqrt{2r}} + O(1)$$

where σ_y is the normal, and τ_{xy} the tangential component of the stress in the plate having a circular hole and crack. Substituting from (3.3) and (3.1) for μ_i,

$$\frac{k_i}{\pi\sqrt{2l(2+\varepsilon^\circ)}} I_k^{(i)} + \sum_{n=0}^{m} a_n^{(i)} I_n^{(i)} = \Lambda_i^{(p)}$$
$$I_k^{(i)}(\xi,\eta) = \int_0^1 M_i \frac{d\eta}{\sqrt{1-\eta}}, \quad I_n^{(i)}(\xi,\eta) = \int_0^1 \eta^n\sqrt{1-\eta}\,M_i\,d\eta \quad (n=0,1,\ldots) \qquad (3.4)$$

Collocations are used to find the coefficients k_i and $a_n^{(i)}$, i.e., (3.4) is assumed to be satisfied at m + 2 points of the interval $1 \le \xi \le 1+\varepsilon^\circ$. The coefficients are then found by Cramer's rule (see, e.g., [11]). If the numerators in Cramer's expressions are expanded in elements of the first column, the coefficients k_i can be written in the form

$$k_i = \frac{\pi\sqrt{2l(2+\varepsilon^\circ)}}{\Delta^{(i)}}\sum_{j=1}^{m+2}\Lambda_i^{(p)}(\xi_j)\,A_{1j}^{(i)} \qquad (3.5)$$

where ξ_j are the points of collocation, $\Delta^{(i)}$ is the determinant of the system of equations obtained from (3.4), and $A_{1j}^{(i)}$ are the cofactors of the elements of the first row of this determinant.

Using the familiar solutions [12], it may be found that, on the line of the crack, for the type of loading in question (see Section 1),

$$\sigma_y^{(p)} = \frac{1}{2}\left[(p+q)\left(1+\frac{1}{x^2}\right)-(p-q)\left(1+\frac{3}{x^4}\right)\cos 2\alpha\right]$$
$$\tau_{xy}^{(p)} = \frac{1}{2}(p-q)\left(1+\frac{2}{x^2}-\frac{3}{x^4}\right)\sin 2\alpha \qquad \left(x=\frac{1+\lambda\xi}{1-\lambda\xi}\right) \tag{3.6}$$

Using (1.4), (3.5), and (3.6),

$$f_1 = \frac{\pi}{2}\sqrt{2a\varepsilon^\circ}\sum_{j=1}^{m+2}\left(1+\frac{1}{x_j^2}\right)\frac{A_{1j}^{(1)}}{\Delta^{(1)}} \qquad f_2 = \frac{\pi}{2}\sqrt{2a\varepsilon^\circ}\sum_{j=1}^{m+2}\left(1+\frac{3}{x_j^4}\right)\frac{A_{1j}^{(1)}}{\Delta^{(1)}}$$
$$f_3 = \frac{\pi}{2}\sqrt{2a\varepsilon^\circ}\sum_{j=1}^{m+2}\left(1+\frac{2}{x_j^2}-\frac{3}{x_j^4}\right)\frac{A_{1j}^{(2)}}{\Delta^{(2)}} \tag{3.7}$$

where $a = b + l$ is the radius of the circle circumscribed about the flaw.

2. In the present calculations, we shall confine ourselves to the value m = 1 and take $\xi_1 = 0.25$, $\xi_2 = 0.625$, and $\xi_3 = 1$ as the points of collocation. With $\varepsilon^\circ \le 0.4$ ($\lambda < 0.167$), the ratios of the cofactors $A_{1j}^{(i)}$ to the corresponding determinants $\Delta^{(i)}$ can be written up to λ^4 as

$$\begin{aligned}
A_{11}^{(1)}/\Delta^{(1)} &= 0.114 - 0.479\,\lambda + 1.569\,\lambda^2 - 5.132\,\lambda^3 + 15.97\lambda^4\\
A_{12}^{(1)}/\Delta^{(1)} &= 0.032 + 0.131\lambda - 0.569\,\lambda^2 + 1.802\,\lambda^3 - 5.708\,\lambda^4\\
A_{13}^{(1)}/\Delta^{(1)} &= 0.103 - 0.143\,\lambda + 0.463\,\lambda^2 - 1.546\,\lambda^3 + 4.792\,\lambda^4\\
A_{11}^{(2)}/\Delta^{(2)} &= 0.114 - 0.210\lambda + 0.078\,\lambda^2 + 0.006\lambda^3 + 0.010\,\lambda^4\\
A_{12}^{(2)}/\Delta^{(2)} &= 0.032 + 0.074\,\lambda + 0.100\,\lambda^2 - 0.011\,\lambda^3 - 0.006\,\lambda^4\\
A_{13}^{(2)}/\Delta^{(2)} &= 0.103 - 0.062\,\lambda + 0.020\,\lambda^2 - 0.0002\cdot\lambda^3 - 0.009\lambda^4
\end{aligned} \tag{3.8}$$

With $\varepsilon_1^\circ = 0.01$, (3.7) and (3.8) give

$$f_1 = 0.109\sqrt{a}, \qquad f_2 = 0.215\sqrt{a}, \qquad f_3 = 0.003\sqrt{a}$$

As might be expected, the corresponding diagram is virtually the same as the line 4 of Fig. 1, referring to a plate with circular flaws [13].

With $\varepsilon_2^\circ = 0.33$, we get

$$f_1 = 0.436\sqrt{a}, \qquad f_2 = 0.646\sqrt{a}, \qquad f_3 = 0.242\sqrt{a}$$

In this case virtually the same diagram is obtained as for the flaw considered in Section 2, 2b.

Finally, in the case $\varepsilon_3^\circ = 1$, (3.7) gives

$$f_1 = 0.496\sqrt{a}, \qquad f_2 = 0.505\sqrt{a}, \qquad f_3 = 0.483\sqrt{a}$$

which is virtually the same as the diagram for a plate with a crack (curve 1 of Fig. 1), i.e., the hole no longer seriously influences the process of crack development.

LITERATURE CITED

1. M. L. Williams, "On the stress distribution at the base of a stationary crack," J. Appl. Mech., 24, No. 1 (1957).
2. G. R. Irwin, Fracture, Hanbuch Physik, Bd: 6, Springer, Berlin (1958).
3. G. I. Barenblatt, "Mathematical theory of equilibrium cracks appearing under brittle fracture," PMTF (J. Appl. Mech. and Tech. Phys.), No. 4 (1961).
4. G. C. Sih, P. C. Paris, and F. Erdogan, "Crack-tip stress – intensity factors for plane extension and plate bending problems," Trans. ASME, Ser. E. J. Appl. Mech., 29, No. 2 (1962).
5. V. V. Panasyuk, Limiting Equilibrium of Brittle Bodies with Cracks [in Russian], Kiev, Naukova Dumka (1968).
6. V. V. Panasyuk, "On fracture of brittle bodies under plane stress," Prikl. Mekhan., 1, No. 9 (1965).
7. V. V. Panasyuk and E. V. Buina, "Critical stress diagrams for brittle bodies with sharp cavity-crack type flaws," Fiz.-Khim. Mekhanika Materialov, 3, No. 5 (1967).

8. H. F. Bueckner, "Some stress singularities and their computation by means of integral equations," in: "Boundary Problems in Differential Equations,"Univ. Wisconsin Press (1960), pp. 215-230.
9. P. M. Vitvitskii and M. Ya. Leonov, "Extension beyond the elastic limit of a plate with a circular hole," PMTF (J. Appl. Mech. and Tech. Phys.), No. 1 (1962).
10. L. L. Libatskii, "Application of singular integral equations for determining critical stresses in plates with cracks," Fiz.-Khim. Mekhanika Materialov, 1, No. 4 (1965).
11. A. G. Kurosh, Course of Higher Algebra [in Russian], Moscow, Gostekhizdat (1955).
12. N. I. Muskhelishvili, Some Fundamental Problems in Mathematical Theory of Elasticity [in Russian], Moscow, AN SSSR (1954).
13. L. L. Libatskii, "On plotting strength diagrams for a brittle body containing elliptic flaws," Fiz.-Khim. Mekhanika Materialov, 5, No. 3 (1969).